Recirculation Gyres Forced by a Beta-Plane Jet*

STEVEN R. JAYNE

MIT–WHOI Joint Program in Oceanography, Woods Hole Oceanographic Institution, Woods Hole, Massachusetts

NELSON G. HOGG

Department of Physical Oceanography, Woods Hole Oceanographic Institution, Woods Hole, Massachusetts

PAOLA MALANOTTE-RIZZOLI

Department of Earth, Atmospheric and Planetary Sciences, Center for Meteorology and Physical Oceanography, Massachusetts Institute of Technology, Cambridge, Massachusetts

(Manuscript received 24 January 1995, in final form 2 August 1995)

ABSTRACT

A numerical model, with quasigeostrophic and barotropic dynamics, is used to study the forcing of mean flows by an unstable jet. The initially zonal jet has specified shape and transport at the western inflow boundary and is sufficiently intense and narrow that the potential vorticity gradient changes sign, giving rise to barotropic instabilities. The resulting eddies act to smooth the potential vorticity anomalies transported into the domain and produce homogenized regions in which recirculations develop to the north and south of the jet. The intensity of these recirculations, as a function of nondimensional beta, is investigated and a simple kinematic interpretation offered.

1. Introduction

Eddies and their associated fluxes can be essential in determining the character of the mean flow, not only as a source of dissipation, but also as a driving force through nonlinear eddy–eddy and eddy–mean flow interactions. Eddy fluxes of nonpassive tracers such as temperature, salinity, momentum, and potential vorticity can significantly influence the overall dynamics of the system. For example, it has been shown that eddies are necessary to close the momentum balance of the Southern Ocean (e.g., Marshall et al. 1993). Transient eddies are created in the ocean due to instabilities, both barotropic and baroclinic, in the general circulation and this is especially true near intensified western boundary currents. The Gulf Stream region is a prime example, where it has been found that the meandering of the stream results in an increase in the eddy potential and kinetic energy by orders of magnitude along the climatological mean path of the jet (Schmitz et al. 1983). The associated eddy fluxes would be expected to significantly affect the jet dynamics and the surrounding fluid.

A general mathematical setting is the quasigeostrophic framework where, in the Eulerian frame, the mean circulation is driven by an eddy vorticity flux:

$$\bar{\mathbf{u}}\cdot\nabla\bar{q} = -\nabla\cdot\overline{(\mathbf{u}'q')}. \tag{1}$$

For the barotropic, flat-bottomed model considered here, $\mathbf{u} = [u, v] = [-\psi_y, \psi_x]$ is the horizontal velocity vector with the streamfunction given by ψ, the relative vorticity defined by $\zeta = \nabla^2\psi$, $q = \zeta + \beta y$ is the potential vorticity, and β represents the variation in the Coriolis parameter with latitude. Here $\mathbf{u}$ and q are decomposed into time-mean and time-varying quantities, $\mathbf{u}(\mathbf{x}, t) = \bar{\mathbf{u}}(\mathbf{x}) + \mathbf{u}'(\mathbf{x}, t)$ and $q(\mathbf{x}, t) = \bar{q}(\mathbf{x}) + q'(\mathbf{x}, t)$, with the overbar denoting the mean and the prime, the deviation from it. To the lowest order Eq. (1) linearizes to

$$\beta\bar{v} = -\nabla\cdot\overline{(\mathbf{u}'q')}, \tag{2}$$

the "eddy Sverdrup relation." The use of a barotropic model to examine the recirculation gyres is motivated by evidence that at least the northern recirculation gyre is strongly barotropic in nature (Richardson 1985; Bower and Hogg 1996).

In a study of the response of a homogeneous ocean to forcing by an oscillatory localized wind stress, Haid-

* Woods Hole Oceanographic Institution Contribution Number 8943.

Corresponding author address: Steven Jayne, Woods Hole Oceanographic Institution, Clark 3, Woods Hole, MA 02543-1541.
E-mail: surje@pimms.mit.edu.

vogel and Rhines (1983) sought the cause of the recirculation gyres seen in the two-layer quasigeostrophic models of Holland and Rhines (1980). In the case of a periodic model, they found that the oscillating source of potential vorticity created a recirculation embedded in a continuous streaming flow to the east. In this case, the contours of potential vorticity closed on themselves. When the domain was closed, however, the potential vorticity contours were blocked, no jet could form, and the recirculation gyres were forced to close at the western boundary. The time-mean flow in this case still exhibited two recirculation gyres, but they were weaker in strength than in the periodic case by a factor of approximately 3, corresponding to the number of times the long wavelength Rossby waves propagate through the periodic domain before decaying from bottom friction (Haidvogel and Rhines 1983). They determined that the mean circulation was driven by a clear relation to potential vorticity fluxes and was less related to Reynolds stresses.

Cessi et al. 1987 (see also Ierley and Young 1988) prescribed the potential vorticity forcing in a different manner. Using barotropic dynamics in a rectangular domain they studied the steady-state solutions arising when a potential vorticity anomaly was specified along the boundary. This was meant to mimic the effect of a western boundary current carrying low potential vorticity water northward from more southerly latitudes. They were able to relate the intensity of the recirculation, and the value of the potential vorticity which was homogenized within it, to the prescribed potential vorticity anomaly. For reasonable values of the anomaly reasonable recirculation strengths and sizes were obtained.

Malanotte-Rizzoli et al. (1995) examined whether forcing a homogeneous ocean by a meandering boundary could produce recirculation gyres in a periodic channel. Similar to the results of Haidvogel and Rhines (1983) for a periodic zonal channel, they found that a streaming flow developed along the eddy-producing region and circulated through the periodic domain. The addition of "sponges" to close the domain removed the streaming circulation, and a weak recirculation was seen: weak, perhaps, because there was no anomaly of potential vorticity to flux away from the boundary as in Cessi et al. (1987). A bowl-shaped topography was added to the model to mimic the sharp thermocline displacement across the Gulf Stream front and the bottom topography north of it. This resulted in closed potential vorticity contours and the creation of a strong recirculation gyre that had a transport of the order of magnitude observed in the Gulf Stream system, although the strength of the recirculation is entirely dependent on the strength of the dissipation.

Observational work in the Gulf Stream seems to be consistent with the numerical predictions. Hogg (1993) measured velocities and temperatures in the Gulf Stream at two moored array sites, one near 55°W and the other near 63°W. Fitting a statistical model to the data, he found the spatial correlation function to be homogeneous and isotropic, leading to a functional relation between the eddy variances and potential vorticity flux divergences. Using the linearized barotropic vorticity equation (2), it was shown that the eddy fluxes were capable of forcing recirculation gyres of 40 Sverdrups (Sv $\equiv 10^6$ m^3 s^{-1}), which is the observed order of magnitude.

In this study we combine many of these ideas. As an extension of the work by Haidvogel and Rhines (1983) and Malanotte-Rizzoli et al. (1995), we seek to force an eddy field to study the time-mean (rectified) current that is produced. However, instead of using an external forcing function, we will use an unstable jet as the eddy source, a jet that transports anomalous values of potential vorticity into the domain rather than prescribing them along the boundary as in Cessi et al. (1987). This setting is more physically representative of currents that have recirculation gyres in the ocean and will lend itself to the statistical analysis used in Hogg (1993).

Conceptually, this study is quite similar to the recent work of Spall (1994), who numerically investigated the effects of instabilities of a deep western boundary current on forcing mean flows. However, Spall's current was meridional: the model contained three layers and bottom relief. This bottom topography, which simulated the continental rise, abyssal plain, and Mid-Atlantic Ridge of the Brazil Basin, played a fundamental role.

2. The model

A quasigeostrophic, homogeneous ocean on a beta plane is considered in our model, for which the vorticity conservation equation is

$$\frac{d\zeta}{dt} + J(\psi, \zeta + \beta_{\text{dim}} y) = -R\zeta, \quad \zeta \equiv \nabla^2\psi, \quad (3)$$

where R is the bottom friction coefficient with units of inverse time. This equation is numerically integrated in time and space using a finite-difference scheme centered in both space and time. A uniform grid spacing of 15 km is used for the spatial differencing on a rectangular grid that is 6000 km long in the zonal direction and 3000 km wide in the meridional direction. The computational mode associated with the time centered, or leapfrog scheme, is suppressed using a time-averaging filter (Haltiner and Williams 1980; Robert 1966). The nonlinear advective terms are handled using the vorticity-conserving scheme devised by Arakawa (1966). At each time step the relative vorticity is inverted to find the streamfunction using the generalized Buneman algorithm (Adams et al. 1988). A zonal jet is imposed as a boundary condition on the eastern and western boundaries in the inversion, and no normal flow is allowed on the northern and southern boundaries. This jet has a Gaussian shape, which gives

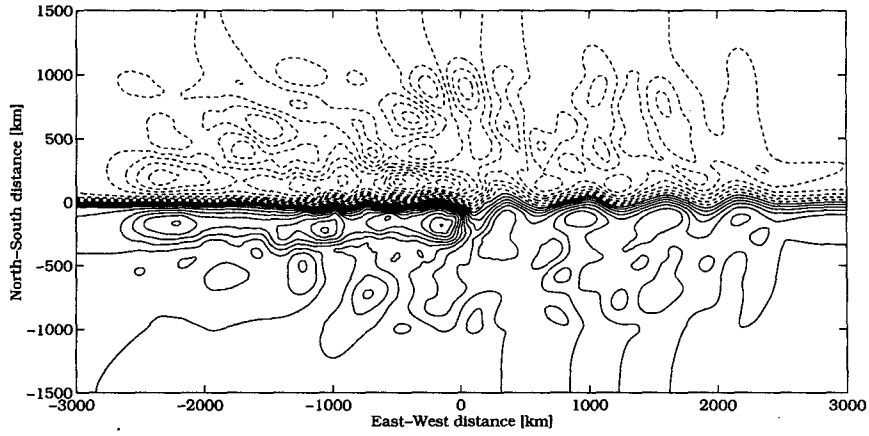

FIG. 1. Instantaneous ψ at model time 20 years with parameters $\beta = 0.05$ and $R_{\text{interior}} = 8.1 \times 10^{-4}$. Contour interval is 5000 m^2 s^{-1}. Negative values are dashed and positive ones are solid lines.

a streamfunction profile of $\psi = (-S)\text{erf}(y/L)$, where S is the strength of the streamfunction and L the half-width of the jet. The interior of the model domain is initialized with the imposed jet plus a Gaussian distributed noise of strength $10^{-3}S$. Dissipation is in the form of $-R\nabla^2\psi$, where R varies from (900 days)$^{-1}$ in the model domain to (1 day)$^{-1}$ in sponge layers that are matched to the boundary flow at the eastern and western boundaries and to no flow on the northern and southern boundaries. The sponges are ramped up linearly from the background value to the maximum value over 32 grid points. Additionally, the dissipation term is treated semi-implicitly (Haidvogel and Rhines 1983).

Nondimensionalizing the vorticity equation gives two free parameters in the model: the dissipation strength, which scales as RL^2/S, and the nondimensional β, which scales as $\beta_{\text{dim}}L^3/S$. The cutoff value for nondimensional β below which instability can occur is where $q_y \equiv \beta - u_{yy}(y, 0) \geq 0$, or $\beta_c = 1.007$, while the Gulf Stream has a value for nondimensional β in the range of 0.02–0.13 (Flierl et al. 1987). The jet that we consider is barotropically unstable leading to a temporal evolution of meanders that are strongly nonlinear. The instability also widens the instantaneous jet profile. By examining cross-stream profiles in the eastern section of the domain, it was empirically found that the jet equilibrates closely to the marginally stable jet so that the nondimensional $\beta \approx \beta_c$ near the outflow. Therefore, to allow the jet to leave the domain in a smooth manner, we impose a wider jet as the outflow boundary condition and determine the half-width of the outflow jet from β_c so that it is marginally stable.

The time-dependent and time-mean dynamics of the jet is strongly affected by our choice of domain size, jet speed, and sponge strength. In particular strong sponges are necessary to suppress the production of a large amplitude stationary meander in the jet. The dynamics of the stationary meander appears to be established by an integer number of wavelengths fitting in the domain. The wavelength can be roughly calculated by following the analysis of the time-dependent evolution of a jet axis by Robinson and Niiler (1967) and Robinson et al. (1975), where the linearized stationary wave equation gives a wavenumber

$$k = \left(\frac{\beta\langle V\rangle}{\langle V^2\rangle}\right)^{1/2}, \tag{4}$$

where $\langle V\rangle = \int V d\eta$ and $\langle V^2\rangle = \int V^2 d\eta$; V is the downstream velocity and η is the cross-stream coordinate. This relation does not hold exactly since the stationary meander is finite in amplitude and its calculation is complicated by the adjoining recirculation gyres. For a combination of wavelength and domain length that does not allow a quantization of the wavenumber, an unstable quasi-stationary meander is produced that periodically shifts by half a wavelength, thus effectively removing the time-mean signature of the meander but not its eddy signature. This stationary meander produces large spatial correlations and long time correlations (order 1000 km and 100 days) for points throughout the domain. We deemed this situation unrealistic, since jets in the ocean do not show strong stationary meanders or similarly strong correlations. Therefore, we restrict ourselves to a parameter range with strong sponges at the boundaries that significantly suppress the stationary wave while allowing for the instability to create strong eddies in the interior of the domain. Apart from suppressing the stationary wave, the sponges do not change the qualitative nature of the recirculation gyres, and only marginally affect their strength. In a much smaller, circular domain, Sakai (1986) has explored these resonances, which in his case, happen at basin scales because the basin is so small and take the form of vortices and stationary waves.

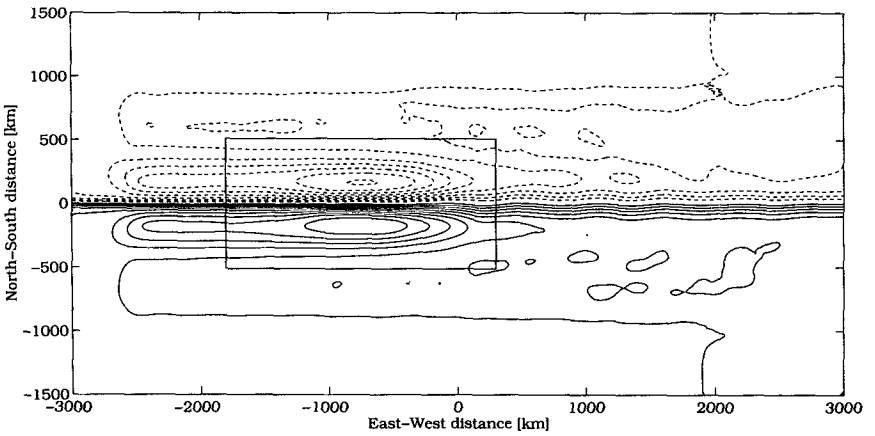

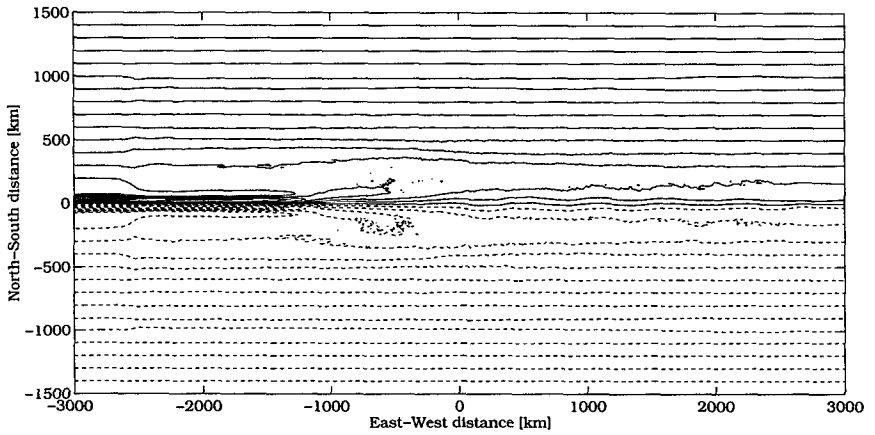

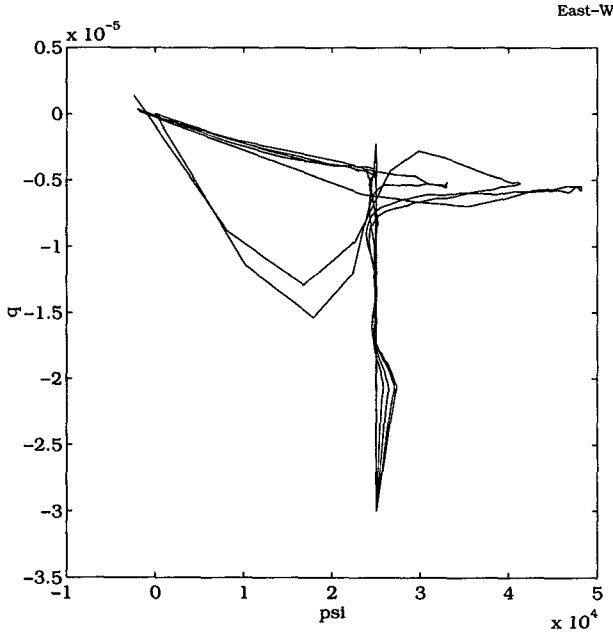

FIG. 2. (a) Mean ψ for model years 11–20 with parameters: $\beta = 0.05$ and $R_{\text{interior}} = 8.1 \times 10^{-4}$. Contour interval is 5000 $m^2\ s^{-1}$. Solid lines are positive and dashed lines are negative values of ψ. Box indicates the area enlarged in Fig. 4. (b) Mean q for model years 11–20. Contour interval is 2 $\times 10^{-6}\ s^{-1}$. Solid lines are positive values and dashed lines are negative. (c) Mean ψ vs mean q at various longitudes within the domain for the northern half of the domain.

The sensitivity of the model was investigated using higher resolution and larger domains. These integrations showed no qualitative change and very little quantitative change in the results. Varying the strength of the sponges and the interior dissipation only changed the recirculation strength slightly while resulting in no significant qualitative change in the recirculation gyres.

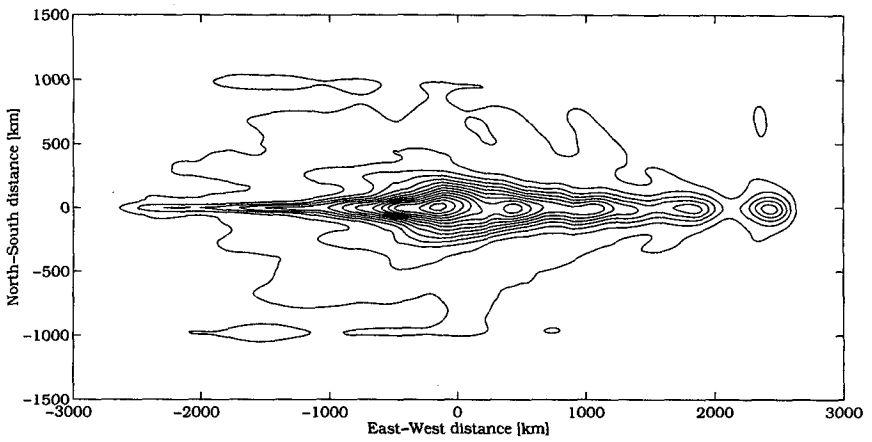

FIG. 3a. $\overline{\psi'\psi'}$. Contour interval is 2.5×10^7 m^4 s^{-2} with parameters: $\beta = 0.05$ and $R_{\text{interior}} = 8.1 \times 10^{-4}$.

3. Model results

We consider the model with the following parameters:

$$\beta_{\text{dim}} = 2 \times 10^{-11} \text{ (m s)}^{-1}$$

$$S = 25\,000 \text{ m}^2 \text{ s}^{-1}$$

$$L = 40 \text{ km}$$

$$R_{\text{interior}} = (900 \text{ days})^{-1}$$

$$R_{\text{sponge}} = (1 \text{ day})^{-1},$$

which gives $\beta = 0.05$, $R_{\text{interior}}L^2/S = 0.00081$, and $R_{\text{sponge}}L^2/S = 0.73$. This set of parameters is chosen to provide an unstable, energetic jet and a sponge strength sufficient to suppress the stationary meander. The numerical model is first integrated for the equivalent of 10 years to spin up, which allows the dynamic fields to come into equilibrium. The run is successively continued for an additional 10 years to allow the computation of mean and eddy fields.

Figure 1 gives the instantaneous streamfunction at 20 model years, showing large meanders and the eddy field produced by jet. The barotropic instability in the jet, clearly evident in Fig. 1, is due to the change in sign of the meridional gradient of potential vorticity and results in the growth of meanders. Figure 2a shows the time-mean streamfunction. We see a stream carrying a transport of 250 Sv if spread over a depth of 5000 m or 50 Sv over 1000 m. We also see two large recirculation gyres on either side of the stream, each of these gyres carrying a transport equivalent to that of the jet itself, consistent with the results of Hogg (1992). Each of these gyres has two parts, one of which recirculates entirely within the domain and the other in which westward flow is returned toward the jet within the sponge layer where a frictional western boundary current is set

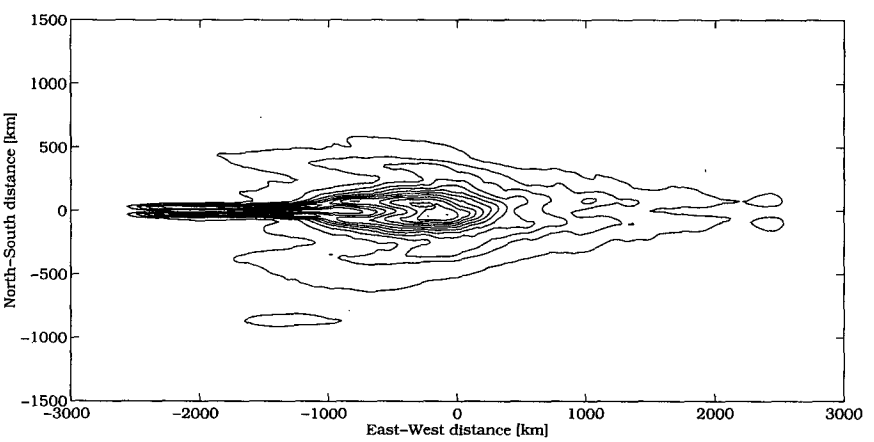

FIG. 3b. $\overline{u'u'}$. Contour interval is 0.002 m^2 s^{-2}.

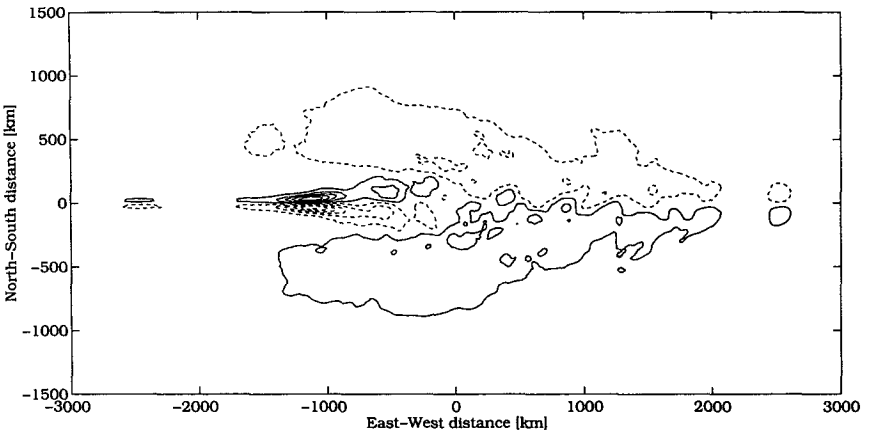

FIG. 3c. $\overline{u'v'}$. Contour interval is 0.001 $m^2 s^{-2}$. Solid lines are positive values and dashed lines are negative.

up. The mean potential vorticity field is shown in Fig. 2b, and we note that the recirculation gyres are located over areas where the potential vorticity is more or less homogenized, as expected (Rhines and Young 1982; Holland et al. 1984). The potential vorticity anomalies are advected eastward but diminish in strength because of the eddy fluxes associated with the instabilities and finally get swept out into the recirculation gyres before being completely dissipated. Figure 2c shows the scatterplot for the mean ψ and q fields. We note the strongly linear relation between ψ and q in the central area of the plot, which corresponds to the jet region in the model. The horizontally flattened sections at the extremity of the plot correspond to the northern recirculation gyre where q is homogenized and ψ reaches its extreme value. The vertically flattened sections correspond to the quiescent region to the north of the jet and the gyre where the planetary β is solely responsible for changing the potential vorticity.

The eddy fields, computed using the relation that $\overline{A'B'} = \overline{AB} - \overline{A}\,\overline{B}$, are shown in Figs. 3a–d and reveal a rich spatial variation. Most prominent is the cigar-shaped region of high streamfunction variability in the center of the domain (Fig. 3a). The velocity covariance terms are also maximal in this region (Figs. 3b–d).

Focusing on the recirculation region (Fig. 4a), we see that the eddy flux of potential vorticity (Fig. 4b) and its divergence (Fig. 4c) are maximum upstream of the area of the most intense eddy activity where the barotropic instability is removing the potential vorticity extrema. It is also the region where the Reynolds stress term $\overline{u'v'}$ (Fig. 3c) has its maximum amplitude and where there is intense, short timescale variability as revealed in the Hovmoeller diagram (Fig. 5a). In the actively unstable region the disturbances propagate rapidly downstream. As the stream stabilizes, the sense of phase propagation reverses, although the group velocity continues to be eastward.

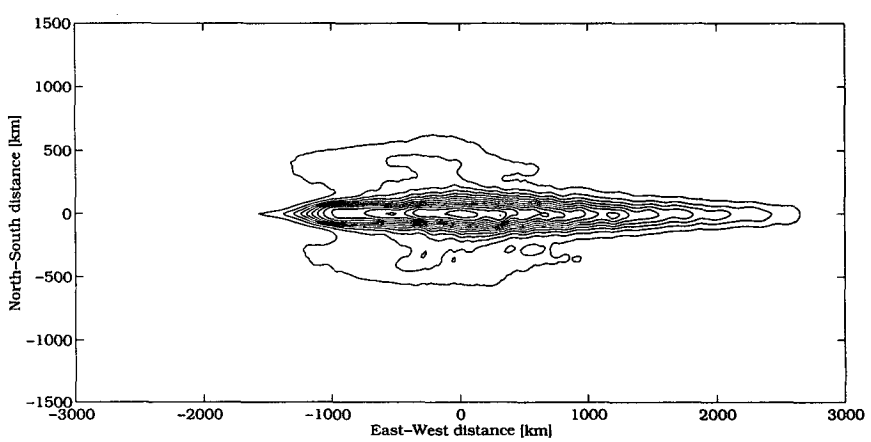

FIG. 3d. $\overline{v'v'}$. Contour interval is 0.002 $m^2 s^{-2}$.

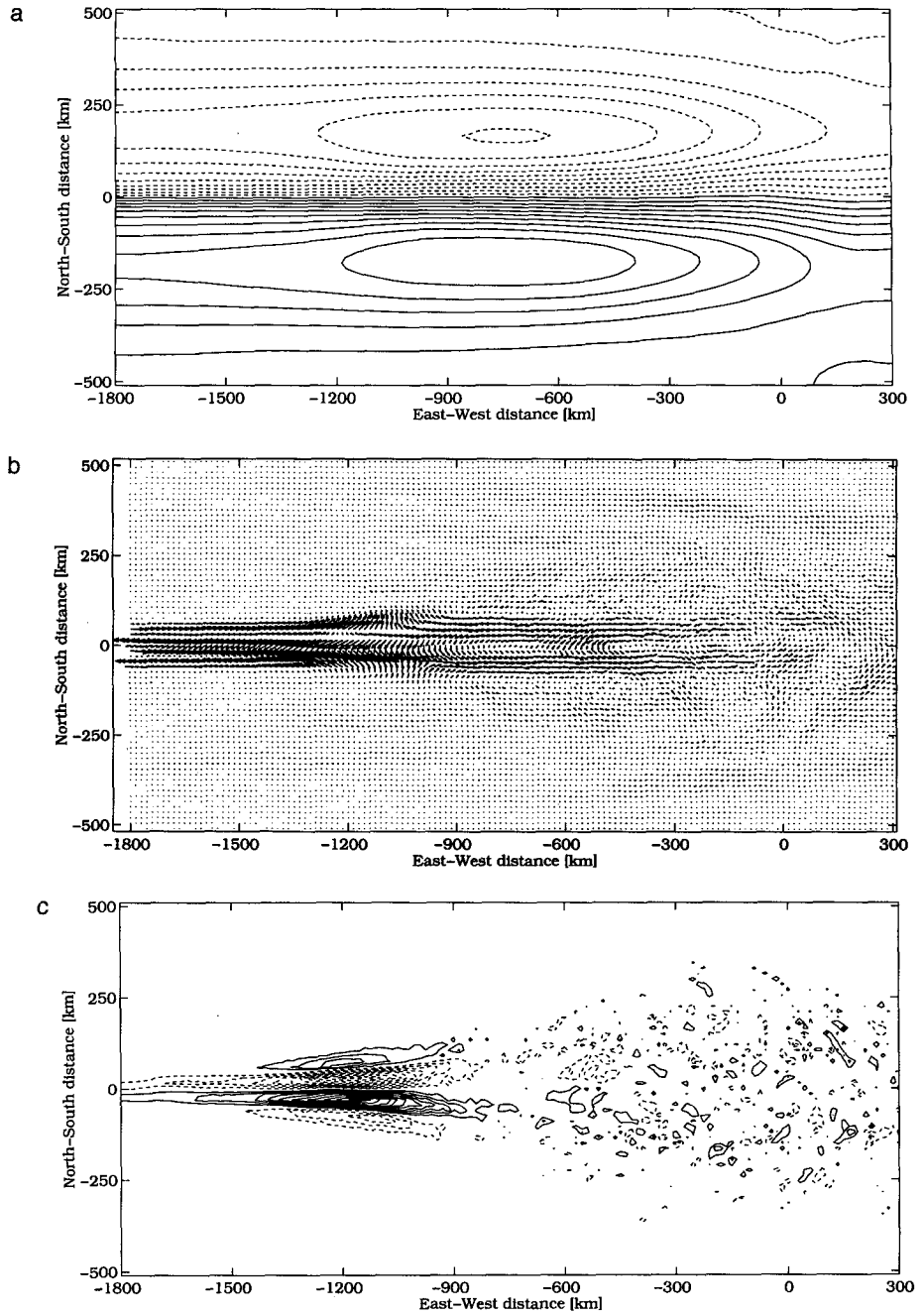

FIG. 4. (a) Mean ψ for enlarged area of Fig. 2a. Contour interval is 5000 m^2 s^{-1}. Solid lines are positive values; dashed lines are negative. (b) $\overline{u'q'}$ for enlarged area. (c) $\nabla\cdot(\overline{u'q'})$ for enlarged area. Contour interval is 1×10^{-12} s^{-2}. Solid lines are positive values; dashed lines are negative.

Away from the jet at $y = 750$ km, (Fig. 5b) the time evolution of ψ is quite different: we see only westward phase and eastward group propagation by waves radiated from the jet.

The dependence of the recirculation strength on β is shown in Fig. 6. We define a nondimensional recirculation index T as the mean recirculating transport divided by $2S$ (S is one-half of the jet transport). A T of unity would mean that each of the recirculation gyres carries a transport equivalent to that of the jet. A T of one-half means that the combined transport of the recirculation gyres is equal to that of the jet. The strength decreases by about 20% over a change of one order of magnitude in β. At values of $\beta > \beta_c$ there is no insta-

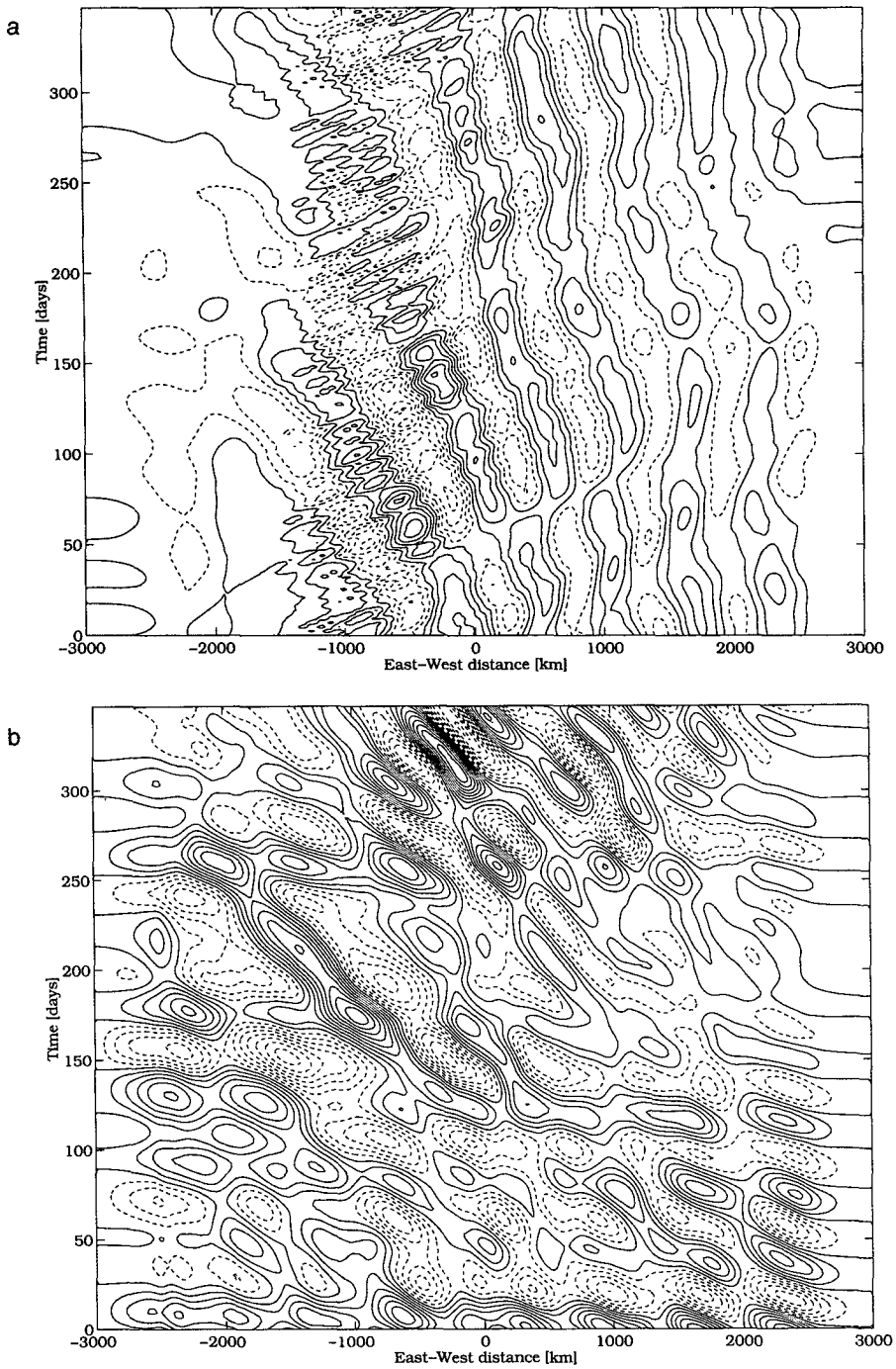

FIG. 5. (a) ψ along line $y = 0$ km for model year 20. Contour interval is 10 000 m^2 s^{-1}, solid lines are positive values of ψ, and dashed lines are negative values of ψ. (b) ψ along line $y = 750$ km for model year 20. Contour interval is 5000 m^2 s^{-1}, solid lines are values of ψ greater than 25 000 m^2 s^{-1}, and dashed lines are values of ψ less than 25 000 m^2 s^{-1}.

bility and, consequently, no eddy field to force recirculation.

There is some sensitivity of T to the value of the interior friction, parameter, R_{interior}. The upper solid curve in Fig. 6a was computed using essentially no interior friction, and the strength of the recirculation falls with increasing β and vanishes at $\beta = 0.9$, just below the value of $\beta_c = 1.007$. At a particular value of

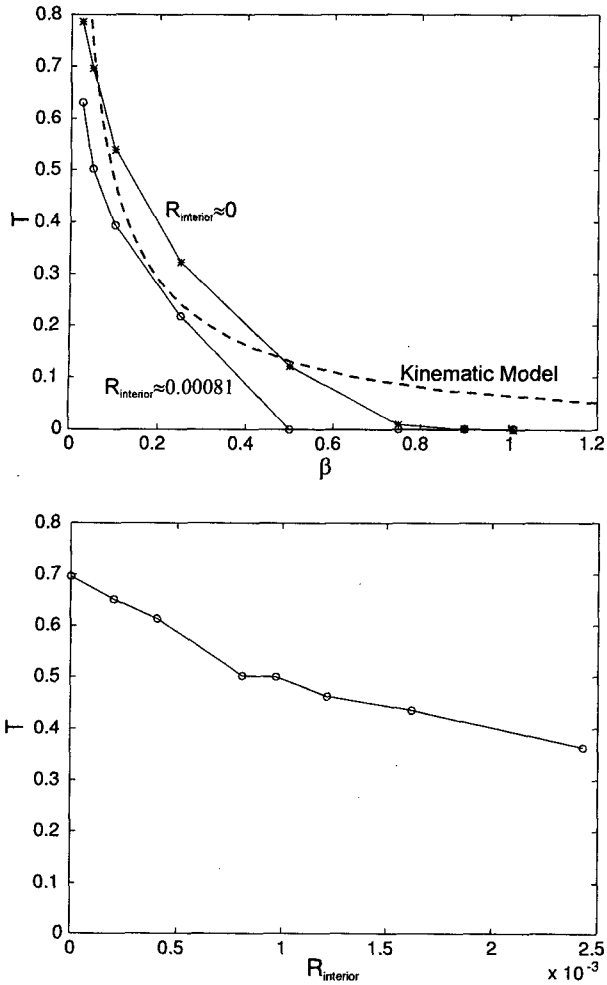

FIG. 6. (a) Nondimensional recirculation strength vs nondimensional β for model results (solid) and predicted by Eqs. (9) and (10) (dashed). The upper solid curve is for vanishing interior friction, $R_{\text{interior}} \approx 0$, whereas the lower solid curve uses $R_{\text{interior}} \approx 8.1 \times 10^{-4}$. (b) Recirculation strength vs bottom friction for the case $\beta = 0.05$.

$\beta = 0.05$, our "standard case," Fig. 6b shows the dependence of T on R_{interior}: it decreases by a factor of 2 when $R_{\text{interior}} \approx 2.5 \times 10^{-3}$, corresponding to a bottom friction of 300 days^{-1}. The lower solid curve in Fig. 6a was determined using a bottom friction of 900 days^{-1}: here the recirculation vanishes for $\beta > 0.5$.

4. Discussion of model results

The primary difference between the results presented here and those of Haidvogel and Rhines (1983) is the form of the forcing used to drive the eddy field. In their study, the source of the eddy field was a time-varying, spatially localized wind stress, whereas our study utilizes an unstable jet. Our eddy variance has a shape and intensity similar to that observed in the Gulf Stream (Schmitz et al. 1983; Hogg 1993): most notable is that the zonal variation scale is much larger than the meridional scale. The forcing used by Haidvogel and Rhines (1983) yields an eddy field whose variability has similar zonal and meridional lengthscales.

Malanotte-Rizzoli et al. (1995) also specified the forcing in a barotropic model. By including just the northern half of the domain and having the southern boundary mimic the meridional velocity of traveling, evolving meanders they found reasonable agreement between the observed and modeled covariances. However, they were only able to obtain a reasonable recirculation strength if the bottom topography was deformed to give closed potential vorticity contours. This feature was motivated by the work of Hogg and Stommel (1985), who suggested that the combination of the real bathymetric slope and the shape of the thermocline results in closed potential vorticity contours for the subthermocline layer. In our model, in which the forcing of the mean flow arises through instability of the jet, closed potential vorticity contours result from the homogenization produced by the resulting eddy fluxes and the recirculation gyres arise more naturally.

As noted above, there are some qualitative similarities between this simple barotropic model and observed variability near the Gulf Stream. In addition to the low aspect ratio, the prominent maximum in eddy energy (Figs. 3b and 3d) is aligned with the jet axis and reaches a maximum well downstream of the "inlet," although the distance suggested by the model, some 3000 km, is somewhat greater than it is in the real world. The intensity of this maximum, approximately 750 cm^2 s^{-2}, is similar in a depth-integrated sense to observed values of 3000 cm^2 s^{-2} near the surface and 200 cm^2 s^{-2} below the thermocline. Finally, the structure in the Reynolds stress term, $\overline{u'v'}$ (Fig. 3c), resembles the classic pattern (e.g., Schmitz et al. 1983) with a change in sign across the axis of the stream. However, for this latter field the model is somewhat richer in structure than the conventionally accepted (and undersampled) Gulf Stream pattern. Within the recirculation zone (i.e., a few hundred kilometers of the axis) there is a checkerboard pattern: to the west of the energy maximum the $\overline{u'v'}$ changes from positive to negative going from south to north while to the east of the energy maximum the opposite is true. Farther from the axis we see wings of negative $\overline{u'v'}$ spreading to the northwest and positive values to the southeast, the expected distribution produced by Rossby wave radiation from an unstable stream (Hogg 1988) and quite evident in the Hovmoeller diagram of Fig. 5b.

Some of these features can be interpreted in terms of a statistical model proposed by Hogg (1993) and inspired by current meter observations near the Gulf Stream. Consistent with these data the spatial covariance function for streamfunction perturbation is proposed to be "quasi homogeneous and quasi isotropic" in the sense that the normalized covariance function is both homogeneous and isotropic:

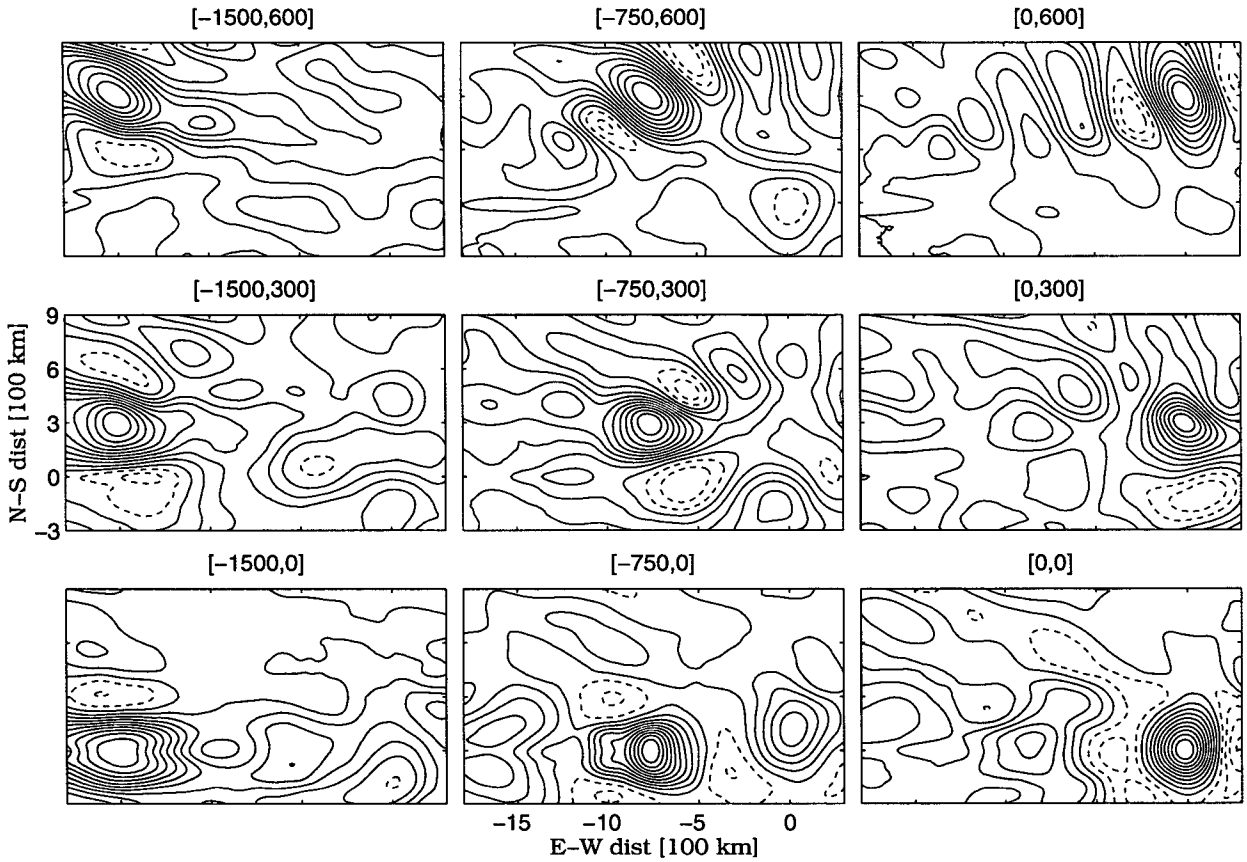

FIG. 7. Normalized spatial correlation functions for various points in the enlarged domain. Contour interval is 0.1. Titles refer to the corresponding point the spatial correlation is calculated from. See Fig. 4 for the corresponding mean and eddy fields. Dashed contours are negative and the interval is 0.1.

$$\overline{\psi'(\mathbf{x}_1)\cdot\psi'(\mathbf{x}_2)} = V(\mathbf{x}_1)V(\mathbf{x}_2)f(|\mathbf{x}_2 - \mathbf{x}_1|), \quad (5)$$

where $V^2(\mathbf{x}) = \overline{\psi'(\mathbf{x})\cdot\psi'(\mathbf{x})}$. With the further assumption that motions are quasigeostrophic (especially true for the model) all the velocity covariances as well as the vorticity fluxes and divergences can be derived from the streamfunction covariance (Bretherton et al. 1976). These relations are

$$\left.\begin{aligned} \overline{u'u'} &= -V^2(\mathbf{x})f''(0) + V_y^2 \\ \overline{v'v'} &= -V^2(\mathbf{x})f''(0) + V_x^2 \\ \overline{u'v'} &= -V_xV_y \end{aligned}\right\}. \quad (6)$$

The "quasi-homogeneous, quasi-isotropic" assumption is approximately obeyed in the model. Figure 7 shows calculations of the normalized spatial covariance function, $f(|\mathbf{x}_2 - \mathbf{x}_1|)$, at various locations in the recirculation region of the model. Although both anisotropy and inhomogeneity are evident, all locations show a dominant central high, which is reasonably circular and decays over a scale of about 175 km (a Gaussian with decay scale of 150–200 km is a good representation). At the more northerly locations, the periodic nature of the radiating Rossby waves asserts itself and produces the positive and negative lobes adjacent to the central high. Figure 8 shows the actual covariance fields and those calculated from Eqs. (6) for an expanded region within the recirculation zone. There is good qualitative similarity although the amplitude for $\overline{u'v'}$ is much too low for the derived field. We can see that the "checkerboard" pattern for this quantity arises from the product of mixed derivatives in (6). The valley in $\overline{u'u'}$ aligned with the jet axis to the west of the maximum is also captured by the statistical model in which it arises from the vanishing of the V_y term at $y = 0$ km.

Using this statistical model Hogg (1993) went on to calculate the strength of the recirculation in the absence of a jet in which case the mean potential vorticity balance reduces to the eddy Sverdrup relation (2). The inclusion of a jet introduces important nonlinear advection terms to the balance and renders this approach less useful.

There are good physical explanations for these characteristics of the variance fields as well: Already

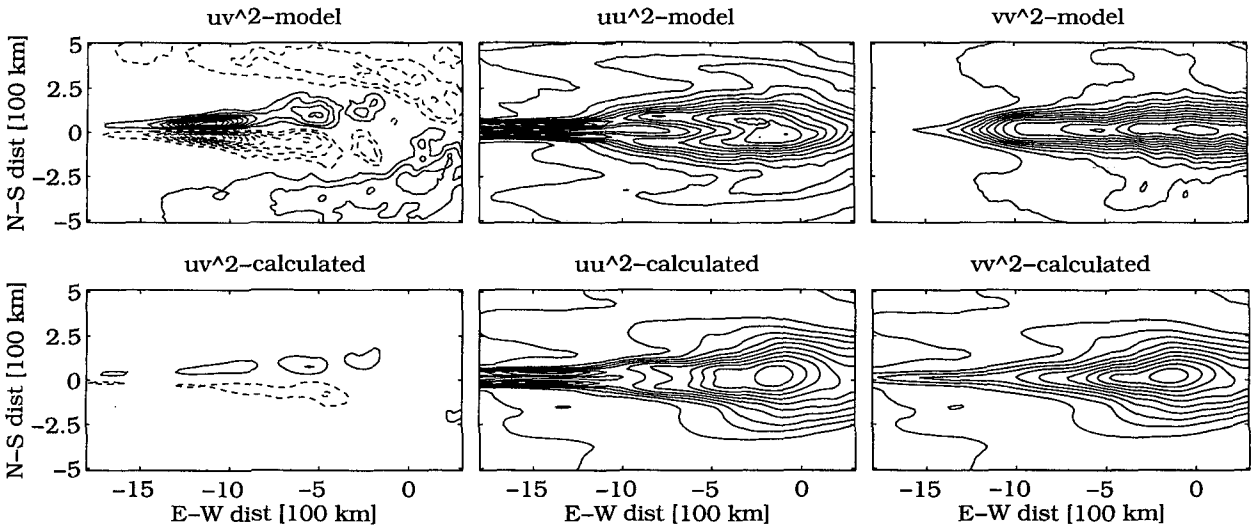

FIG. 8. Covariance fields from the model and those predicted by Eq. (6).

mentioned is the tendency for Rossby wave radiation to produce the "butterfly wings" of negative and positive values of $\overline{u'v'}$ well to the north and south of the jet. Within the jet the barotropic instability process attempts to smooth the jet profile and the resulting momentum fluxes will be positive on the north and negative on the south, as observed in the upstream region. Finally, where the resulting meanders are still small compared to the jet width, the perturbation of the zonal velocity will be a minimum along the axis where the jet velocity is a maximum.

In a manner analogous to the approaches of Hogg and Stommel (1985) and Cessi et al. (1987), we have been able to construct a simple conceptual model of the time-mean state of our time-dependent model. Figure 9a shows the meridional distribution of potential vorticity for the northern half of the model at selected longitudes. We see the smoothing of the large anomalies found near the western boundary and the development of a plateau of uniform potential vorticity within the recirculation. At this point the potential vorticity can be modeled as three regimes (Fig. 9a):

$$q = \begin{cases} q = \alpha y, & 0 < y < y_0 \\ q_0 = \beta y_m, & y_0 < y < y_1 \\ q = \beta y, & y_1 < y \end{cases} \tag{7}$$

with $\alpha y_0 = \beta y_m$ so that q is continuous at $y = y_0$. Within each of the first two regions the velocity is parabolic in y if we neglect the contribution of the zonal derivative of the meridional velocity to relative vorticity, which, based on model data, is a very good approximation. Matching at y_0 and setting $u(y) = 0$ at the edge of the recirculation, $y = y_1$, gives

$$u(y) = \begin{cases} -(\alpha - \beta)y^2/2 + \beta(2y_m y_1 - y_m y_0 - y_1^2)/2, & 0 < y < y_0 \\ \beta((y - y_m)^2 - (y_1 - y_m)^2)/2, & y_0 < y < y_1 \\ 0, & y_1 < y. \end{cases} \tag{8}$$

There are three unknowns, y_0, y_m, and y_1 representing the edges of the recirculation and the position where the homogenized potential vorticity equals the planetary value (and the recirculation velocity is a maximum). Two conditions are provided by the requirements that the total recirculation transport vanishes and that the normalized jet transport equal that prescribed at the inlet:

$$1 = \int_0^{y_0} u(x, y)dy = (\beta/18)y_0(3y_1 + y_0)(y_1 - y_0)$$

$$0 = \int_{y_0}^{y_1} u(x, y)dy = (y_1 - y_0)^2(3y_m - y_0 - 2y_1)/3; \tag{9}$$

the second of which simplifies to $y_m = (y_0 + 2y_2)/3$. A third and final condition is ad hoc—that the meridionally integrated vorticity anomaly δQ be constant:

$$\delta Q = \int_0^{\infty} (q(y) - \beta y)dy$$

$$= (\beta/6)(y_2^2 - y_0^2) = u(0) = 2/\sqrt{\pi} \tag{10}$$

after being nondimensionalized. These three conditions reduce to a single polynomial of fourth degree, whichcan then be solved. The variation of the recirculating transport with β is shown in Fig. 6 where agreement with the modeled transport is reasonable, especially for values of β well below critical. In Fig. 9b we show, for two values of β, the plots of q versus ψ from both the numerical model and analytic models. For $\beta = 0.05$ we make a comparison in Fig. 10 of the calculated zonal velocity

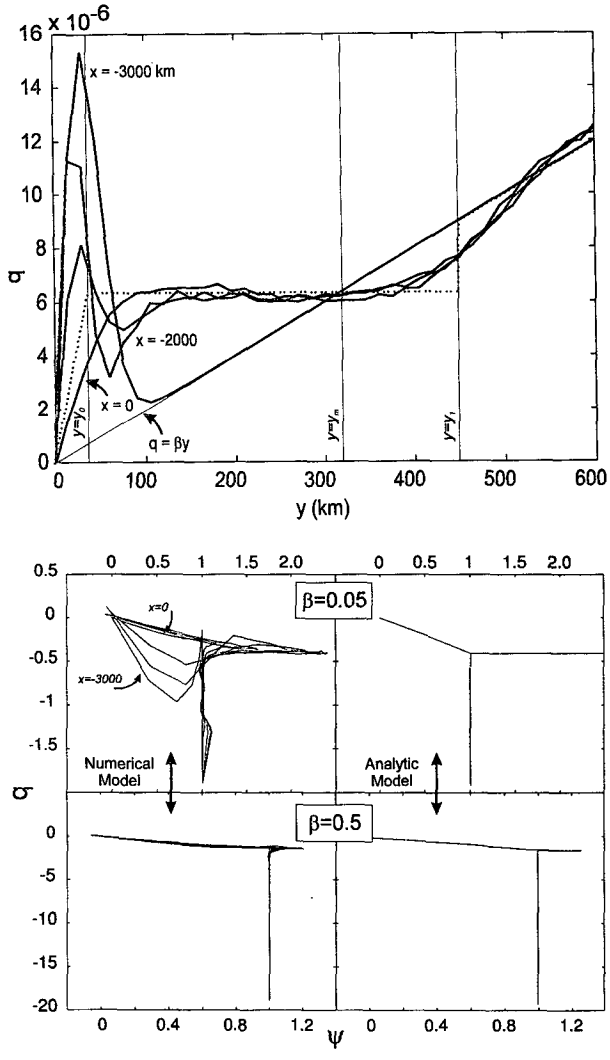

FIG. 9. (a) Meridional distribution of potential vorticity in northern half of the model for selected longitudes (at $x = -3000$ km, -2000 km, -1000 km, and 0 km) for $\beta = 0.05$. Notice the flattening of the profiles toward the line $q = \beta y$ (thin solid line) and the development of a homogeneous plateau. Dotted line gives the distribution of the kinematic model. (b) Distribution of nondimensional q vs ψ for $\beta = 0.05$ (upper panels) and $\beta = 0.5$ (lower panels) giving both numerical model values (left panels) and those predicted by the kinematic model (right panels).

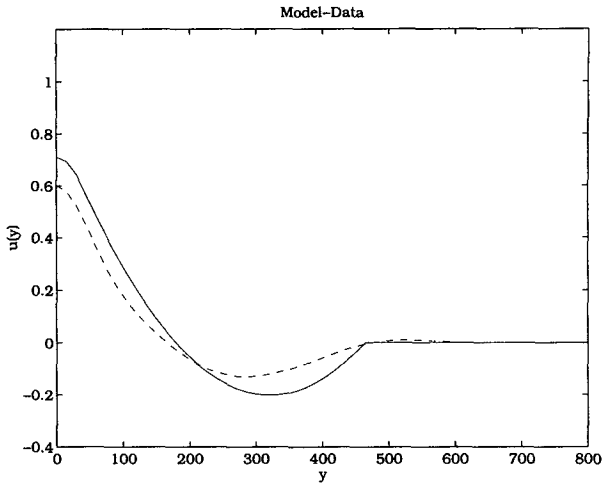

FIG. 10. Mean zonal velocity (solid) and calculated zonal velocity from the kinematic model (dashed).

with the mean from the model at a position near the maximum of the recirculation and again find a reasonable agreement.

5. Conclusions

Inertial western boundary currents such as the Gulf Stream advect low potential vorticity water northward, at least to the extent that advection dominates dissipation. By imposing the jet structure at the western inlet, in our model, we have simulated this feature in a traditional "two gyre" sense with a negative anomaly to the south of the axis and a positive one to the north. If the jet structure is sufficiently intense, such that $\beta < \beta_c$, these anomalies create extrema in the ambient potential vorticity distribution and the jet is barotropically unstable. The resulting disturbances flux potential vorticity in such a way as to smooth out the anomaly and create plateaus of uniform potential vorticity to the north and south of the jet axis in which inertial recirculations form. A simple, piecewise linear model of the mean potential vorticity distribution has reproduced, in a semiquantitative sense, many of the features of this recirculation including the dependence of its strength on β. In the sense of the "eddy Sverdrup relation" [Eqs. (1) or (2)] the recirculation gyres are only weakly forced by the eddies and, instead, are predominantly inertial with the mean vorticity balance being dominated by advection of relative and planetary vorticity. It is unclear to us how these dynamics might survive in a baroclinic jet where baroclinic instability is also possible, and we intend to explore this dimension in the future.

Acknowledgments. This study was supported by the Woods Hole Oceanographic Institution's Summer Student Fellow Program, the Massachusetts Institute of

Technology's Sea Grant College Program through the Undergraduate Research Opportunities Program, and a National Defense Science and Engineering Graduate Fellowship (SRJ), the Office of Naval Research through Grants N00014-85-C-0001 (NGH) and N00014-90-J-1481 (PMR). Comments from Mike Spall and two reviewers were very helpful.

REFERENCES

Adams, J., P. Swartztrauber, and R. Sweet, 1988: FISHPAK: A package of FORTRAN subprograms for the solution of separable elliptic partial differential equations, version 3.2.

Arakawa, A., 1966: Computational design for long-term numerical integration of the equations of fluid motion: Part I: Two-dimensional incompressible flow. *J. Comput. Phys.*, **1,** 119–145.

Bower, A. S., and N. G. Hogg, 1996: On the structure of the Gulf Stream and its recirculations at 55°W. *J. Phys. Oceanogr.*, submitted.

Bretherton, F. P., R. Davis, and C. Fandry, 1976: A technique for objective analysis and design of oceanographic experiments. *Deep-Sea Res.*, **23,** 559–582.

Cessi, P., G. Ierley, and W. Young, 1987: A model of the inertial recirculation driven by potential vorticity anomalies. *J. Phys. Oceanogr.*, **17,** 1640–1652.

Flierl, G. R., P. Malanotte-Rizzoli, and N. J. Zabusky, 1987: Nonlinear waves and coherent vortex structures in barotropic beta-plane jets. *J. Phys. Oceanogr.*, **17,** 1408–1438.

Haidvogel, D. B., and P. B. Rhines, 1983: Waves and circulation driven by oscillatory winds in an idealized ocean basin. *Geophys. Astrophys. Fluid Dyn.*, **25,** 1–63.

Haltiner, G. J., and R. T. Williams, 1980: *Numerical Prediction and Dynamic Meteorology.* 2d ed. Wiley and Sons, 477 pp.

Hogg, N. G., 1988: Stochastic wave radiation by the Gulf Stream. *J. Phys. Oceanogr.*, **18,** 1687–1701.

——, 1992: On the transport of the Gulf Stream between Cape Hatteras and the Grand Banks. *Deep-Sea Res.*, **39,** 1231–1246.

——, 1993: Toward parameterization of the eddy field near the Gulf Stream. *Deep-Sea Res.*, **40,** 2359–2376.

——, and H. Stommel, 1985: On the relationship between the deep circulation and the Gulf Stream. *Deep-Sea Res.*, **32,** 1181–1193.

Holland, W. R., and P. B. Rhines, 1980: An example of eddy-induced ocean circulation. *J. Phys. Oceanogr.*, **10,** 1010–1031.

——, T. Keffer, and P. B. Rhines, 1984: Dynamics of the oceanic general circulation: The potential vorticity field. *Nature,* **308,** 698–705.

Ierley, G. R., and W. R. Young, 1988: Inertial recirculation on a β-plane corner. *J. Phys. Oceanogr.*, **18,** 683–689.

Malanotte-Rizzoli, P., N. G. Hogg, and R. E. Young, 1995: Stochastic wave radiation by the Gulf Stream: Numerical experiments. *Deep-Sea Res.*, **42,** 389–423.

Marshall, J., D. Olbers, H. Ross, and D. Wolf-Gladrow, 1993: Potential vorticity constraints on the dynamics and hydrography of the Southern Ocean. *J. Phys. Oceanogr.*, **23,** 465–487.

Rhines, P. B., and W. R. Young, 1982: Homogenization of potential vorticity in planetary gyres. *J. Fluid Mech.*, **122,** 347–367.

Richardson, P. L., 1985: Average velocity and transport of the Gulf Stream near 55°W. *J. Mar. Res.*, **43,** 83–111.

Robert, A. J., 1966: The integration of a low order spectral form of the primitive meteorological equations. *J. Meteor. Soc. Japan, Ser. 2,* **44,** 237–245.

Robinson, A. R., and P. P. Niiler, 1967: The theory of free inertial currents. Part I: Path structure. *Tellus,* **19,** 269–291.

——, J. R. Luyten, and G. Flierl, 1975: On the theory of thin rotating jets: A quasi-geostrophic time dependent model. *Geophys. Fluid Dyn.*, **6,** 211–244.

Sakai, S., 1986: Vortex flow regime in an inflow–outflow model at mid-latitude. *Deep-Sea Res.*, **33,** 1107–1125.

Schmitz, W. J., Jr., W. R. Holland, and J. F. Price, 1983: Mid-latitude mesoscale variability. *Rev. Geophys. Space Phys.*, **21,** 1109–1119.

Spall, M. A., 1994: Wave-induced abyssal recirculations. *J. Mar. Res.*, **52,** 1051–1080.